

CONTRACTOR REPORT

SAND84-8176

UC-62c

Unlimited Release

Molten Salt Solar Receiver Subsystem Research Experiment — Executive Summary

Foster Wheeler

Prepared by Sandia National Laboratories, Albuquerque, New Mexico 87185
and Livermore, California 94550 for the United States Department of Energy
under Contract DE-AC04-76DP00789.

Printed September 1984

Issued by Sandia National Laboratories, operated for the United States Department of Energy by Sandia Corporation.

NOTICE: This report was prepared as an account of work sponsored by an agency of the United States Government. Neither the United States Government nor any agency thereof, nor any of their employees, nor any of the contractors, subcontractors, or their employees, makes any warranty, express or implied, or assumes any legal liability or responsibility for the accuracy, completeness, or usefulness of any information, apparatus, product, or process disclosed, or represents that its use would not infringe privately owned rights. Reference herein to any specific commercial product, process, or service by trade name, trademark, manufacturer, or otherwise, does not necessarily constitute or imply its endorsement, recommendation, or favoring by the United States Government, any agency thereof or any of their contractors or subcontractors. The views and opinions expressed herein do not necessarily state or reflect those of the United States Government, any agency thereof or any of their contractors or subcontractors.

Printed in the United States of America
Available from
National Technical Information Service
5285 Port Royal Road
Springfield, VA 22161

NTIS price codes
Printed copy: A04
Microfiche copy: A01

MOLTEN SALT SOLAR RECEIVER
SUBSYSTEM RESEARCH EXPERIMENT
- EXECUTIVE SUMMARY

PHASE 1--FINAL REPORT

Prepared for

Sandia National Laboratories
Livermore, California

By

G. Carli
Project Manager

November 1982

Contract 84-2292C
SAND 84-8176
FWSDC No. 9-71-9203

ACKNOWLEDGMENTS

This report was prepared by Foster Wheeler Solar Development Corporation for Sandia National Laboratories, Livermore, with contributions from:

Foster Wheeler Development Corporation:

G. Carli (Principal author)
C. K. Cha
S. J. Goidich
W. F. Kegel
J. G. Rabe (Editor)
M. S. Rao
J. W. Schroeder

Foster Wheeler Energy Corporation:

J. Buren
C. Maffei
J. Miso
D. P. Money
S. F. Gillen

Foster Wheeler Solar Development Corporation:

T. V. Narayanan
S. F. Wu
R. J. Zoschak

Foster Wheeler Special Projects Engineering and Construction, Inc.:

J. E. Jackson
M. P. Kramer

McDonnell Douglas Corporation:

C. R. Cross
W. L. Dreier
C. M. Finch
C. J. Kennedy
T. J. McKeown
G. G. McKhann

CONTENTS*

| <u>Section</u> | | <u>Page</u> |
|------------------------------------|---|-------------|
| <u>VOLUME 1--EXECUTIVE SUMMARY</u> | | |
| | ACRONYMS | v |
| 1 | EXECUTIVE SUMMARY | 1-1 |
| | 1.1 Introduction | 1-1 |
| | 1.1.1 Background | 1-1 |
| | 1.1.2 Project Objective | 1-2 |
| | 1.1.3 Definition of the RS (Receiver Subsystem) | 1-3 |
| | 1.1.4 Technical Approach | 1-3 |
| | 1.1.5 Project Team | 1-7 |
| | 1.2 Selection of the RS | 1-8 |
| | 1.2.1 Trade-Off Studies | 1-8 |
| | 1.2.2 Selected Configuration | 1-10 |
| | 1.2.3 Materials Selection | 1-13 |
| | 1.3 RS Design Analysis | 1-16 |
| | 1.3.1 Design Point | 1-16 |
| | 1.3.2 Thermal/Hydraulic Design Analysis | 1-18 |
| | 1.3.3 Stress Analyses | 1-22 |
| | 1.3.4 Mechanical Design Analysis | 1-25 |
| | 1.3.5 Operation and Control Analysis | 1-26 |
| | 1.4 RS Summary Description | 1-28 |
| | 1.5 Panel Fabrication Development | 1-36 |
| | 1.6 Weight and Cost Estimates | 1-44 |
| | 1.7 Receiver Development | 1-46 |

*Published in three separate volumes. Tables and Illustrations are listed individually for each volume.

ILLUSTRATIONS

| <u>Number</u> | | <u>Page</u> |
|---------------|---|-------------|
| 1.1 | Schematic of RS | 1-4 |
| 1.2 | Absorber Isometric and Circuitry | 1-11 |
| 1.3 | Temperature Profile of Absorber Hottest Tube | 1-19 |
| 1.4 | 320-MW Molten Salt Solar Cavity Receiver | 1-29 |
| 1.5 | RS Flow Schematic | 1-34 |
| 1.6 | Overall View of Welding Set-Up Showing the Welding Head, Wire Reel, Controls, Cross-Beam Carriage, and Pneumatically Actuated Toggle Clamps | 1-37 |
| 1.7 | Cross Section of Welded Panel Tubes | 1-38 |
| 1.8 | Welding of Third Development Panel | 1-41 |
| 1.9 | Support Lug Attachment Methods | 1-41 |
| 1.10 | Third Development Panel Showing Support Lugs at Each End | 1-43 |
| 1.11 | Schematic of the SRE Test Cavity | 1-48 |

TABLES

| <u>Number</u> | | <u>Page</u> |
|---------------|--|-------------|
| 1.1 | Team Responsibilities | 1-7 |
| 1.2 | RS Design Data Summary | 1-17 |
| 1.3 | RS Performance | 1-21 |
| 1.4 | Thermal/Hydraulic Performance Data Summary | 1-23 |
| 1.5 | Configuration Data Summary | 1-30 |
| 1.6 | Receiver Weight | 1-44 |
| 1.7 | Construction Cost Estimate | 1-45 |

ACRONYMS

| | |
|---------|--|
| ACR | Advanced Central Receiver |
| ACR-SRE | Advanced Central Receiver Molten Salt Subsystem Research Experiment |
| AISC | American Institute of Steel Construction |
| ANSI | American National Standards Institute |
| ANSYS | Finite element program for static structural, heat-transfer, thermal, thermal stress, dynamic, seismic, and inelastic analyses. Contains many element types, such as beam, plane stress, axisymmetric solid, axisymmetric shell, general shell, and three-dimensional solid. |
| APS | Arizona Public Service |
| ASME | American Society of Mechanical Engineers |
| CONCEN | MDC code for detailed analysis of receiver flux profiles. Predicts flux profiles for a field layout consisting of individual heliostat locations. Also provides detailed performance analysis (diurnal and annual). |
| CRTF | Central Receiver Test Facility |
| CS | Collector Subsystem |
| GST | Cold Storage Tank |
| DAP | Design Analysis Plan |
| DELSOL | SNLL computer code for quantifying the performance, determining field layouts, and optimizing cost/performance of large central solar receiver systems. |
| DFR | Design Flow Rate |
| DOE | Department of Energy |
| FPDP | Fabrication Process Development Plan |
| FWDC | Foster Wheeler Development Corporation |
| FWEC | Foster Wheeler Energy Corporation |

ACRONYMS (Cont)

| | |
|--------|---|
| FWSDC | Foster Wheeler Solar Development Corporation |
| FWSPEC | Foster Wheeler Special Projects Engineering and Construction, Inc. |
| GTA | Gas Tungsten Arc |
| HAZ | Heat-Affected Zone |
| HST | Hot Storage Tank |
| IST | Inlet Surge Tank |
| MDC | McDonnell Douglas Corporation |
| MIG | Metal Inert Gas |
| MMC | Martin Marietta Corporation |
| MSEE | Molten Salt Electric Experiment |
| NASA | National Aeronautics and Space Administration |
| NRC | Nuclear Regulatory Commission |
| NONAX | FWDC-developed special-purpose program to solve for thick-walled cylinders made of homogeneous and isotropic material under non-axisymmetric loading (loading may consist of an arbitrary combination of internal and external tractions, axial load, axial bending, and an arbitrary temperature distribution). Determines thermoelastic, elastic-plastic, and creep solutions under varying load cycles and hold times. |
| OST | Outlet Surge Tank |
| PCR | Partial Cavity Receiver |
| P&ID | Piping and Instrumentation Diagram |
| QCR | Quad-Cavity Receiver |
| RFQ | Request for Quotation |
| RS | Receiver Subsystem |

ACRONYMS (Cont)

| | |
|--------|--|
| RSS | Root Sum Square Method |
| SCRS | Solar Central Receiver System |
| SINDA | General software system designed primarily for the solution of thermal analog models presented in network format. Can be used as a general-purpose program with its array and constant capability along with library of user subroutines. |
| SNLL | Sandia National Laboratories, Livermore |
| SOLAR | FWSDC-developed program to perform the steady-state thermal/hydraulic analysis of molten salt-cooled solar receivers. Calculates tubewall and salt temperatures at each node location and absorbed power, salt bulk temperature change, and pressure drop for each zone. Calculates variations in flow (flow distribution) among panel tubes caused by variations in heat flux across panel. |
| SPP | Sierra Pacific Power Company |
| SRE | Subsystem Research Experiment |
| TEMA | Tubular Exchanger Manufacturers Association |
| T/H | Thermal/Hydraulic |
| TIG | Tungsten Inert Gas |
| TRASYS | Geometric modeling program that computes the black and gray body view factors and determines the solar and infrared radiation interchange between surfaces in cavity and partial cavity receivers. |
| UBC | Uniform Building Code |
| VDCRP | Voltage, Direct Current Reverse Polarity |

Section 1

EXECUTIVE SUMMARY

1.1 INTRODUCTION

This report presents the results of the work done in Phase 1 of a Department of Energy (DOE)-funded project for developing a cost-effective molten salt Receiver Subsystem (RS) for a commercial-size Solar Central Receiver System (SCRS) and providing the commercial fabrication process development for molten salt receivers.

The report comprises three volumes. Volume 1, the Executive Summary, presents an overview of the study, including major results and conclusions along with a concise description of the RS. Volume 2 presents the discussions, evaluations, and results of work done during Tasks 1 through 7. Volume 3 contains Appendices A through T--detailed analyses and supporting information.

1.1.1 Background

Recent DOE studies have shown that, technically and economically, molten nitrate salt (60 wt% NaNO_3 /40 wt% KNO_3) is one of the leading candidates for a high-temperature, central receiver heat-transfer fluid. The advantages of molten salt include low cost, chemical stability, low corrosion rates, a low melting point, a high usable temperature at a low operating pressure, and high heat capacity for thermal storage. It has been used successfully in process heat applications for many years. However, at the temperature and duty cycle of an SCRS, it has a limited industrial application and data base.

Recognizing the attractiveness of molten nitrate salt, DOE has conducted an extensive program to identify uncertainties and concerns relating to its use and to develop the data base, technology, and hardware components that are essential for the development of a commercial molten salt SCRS.

DOE and Sandia National Laboratories, Livermore (SNLL) have been systematically developing this data base and the technology for SCRS applications. This study is an important element in these activities.

In several recent molten salt SCRS studies, the receiver was studied as a part of the entire plant. Consequently, even though a considerable body of information has been generated, important receiver design, fabrication, and operating issues require additional investigation.

1.1.2 Project Objective

The overall project objective was to design a reliable and cost-effective molten salt RS. Specifically, the project was aimed at resolving all critical design, fabrication, operating, and performance uncertainties.

The work done under this contract (Phase 1) consists of the definition of the requirements specification, the preliminary design of a 320-MW* molten salt RS, and a fabrication development task to resolve any fabrication uncertainties, performed in sufficient detail to achieve the objectives of developing a reliable, cost-effective molten salt RS for a commercial SCRS.

*Thermal unless otherwise specified.

1.1.3 Definition of the RS

The RS, shown schematically in Figure 1.1, provides a means of transferring the incident radiant flux energy from the heliostat field into the molten salt heat-transfer fluid. The RS consists of an elevated receiver to intercept the radiant flux, the tower structure to support the receiver, and the riser and downcomer piping. The RS also includes the pumps, valves, and control system necessary to regulate fluid flow, temperature, and pressure and the required thermal conditioning necessary for its safe and efficient operation, start-up, shutdown, and standby.

The terminal points defining components within the scope of the RS are at the boundary of the tower structure where the riser and downcomer meet the cold and hot salt lines from the Thermal Storage Subsystem. These terminal points were selected so that the RS design is not dependent upon the physical layout of a specific job site.

1.1.4 Technical Approach

The project was divided into 10 tasks. After a review of SNLL's Preliminary RS Specification (Task 1), the RS Requirements Specification was developed (Task 2). Based on these Requirements, technical and economic parametric analyses were performed and a configuration was selected (Task 3). Detailed preliminary design of the RS was made and its performance was evaluated (Task 4). Fabrication and construction plans were prepared and capital costs were estimated (Task 5). Panel fabrication techniques were developed (Task 6), and a development plan for Phase 2 was prepared (Task 7). Following a redirection of

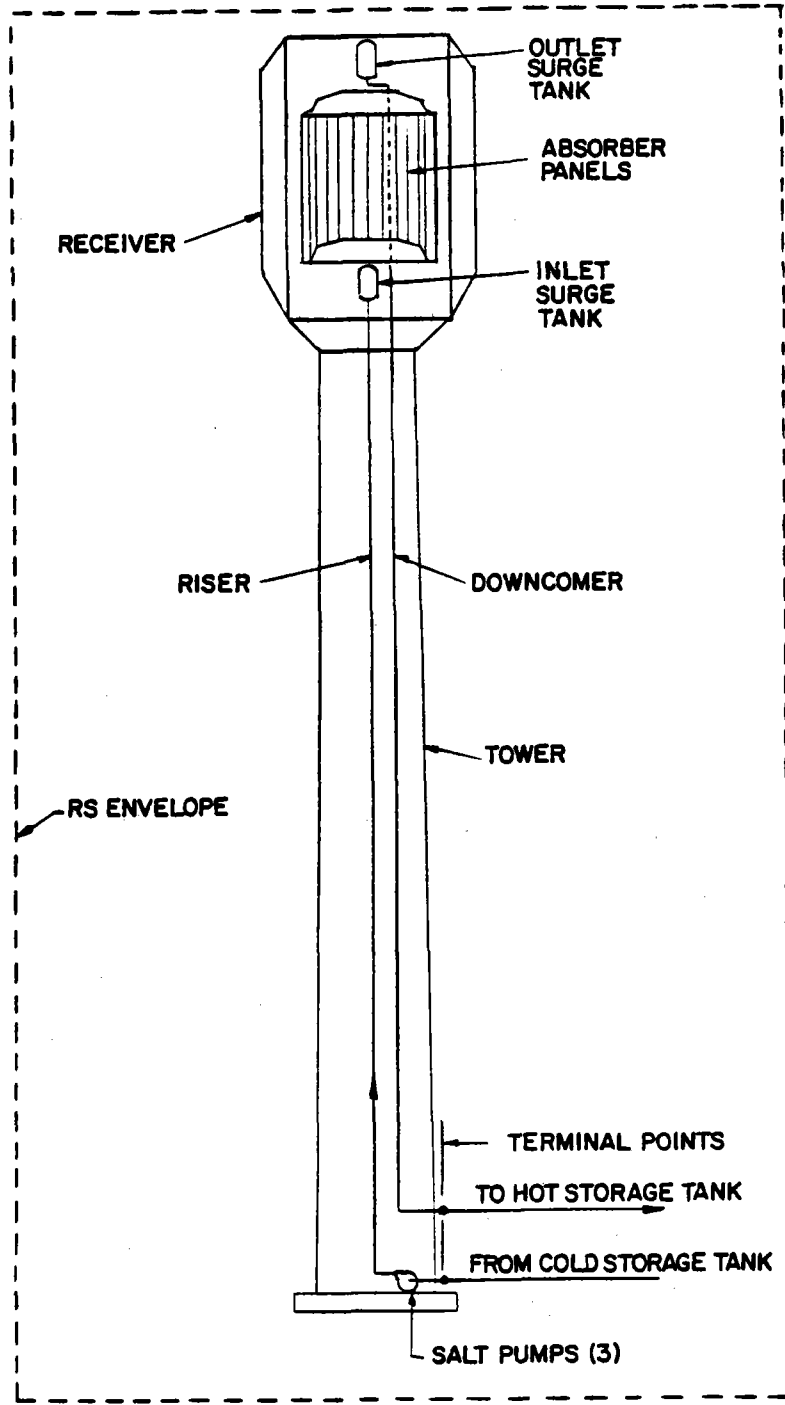


Figure 1.1 Schematic of RS

effort by SNLL, the Phase 2 proposal (Task 8) was deleted. Task 9 consisted of reports and meetings; Task 10, project management and administration. The contract period of performance was from September 1981 through November 1982. An outline of the contract Statement of Work follows.

Task 1--Review of RS Specification

- Review Molten Salt Subsystem Specification given by SNLL
- Submit changes to SNLL within 15 days after authorization to proceed
- Update specifications, if necessary, as work proceeds.

Task 2--Definition of RS Requirements

- Review literature on molten salt, molten salt receivers, and salt-based solar central receiver plants
- Develop system-level requirements specification for the RS.

Task 3--RS Concept Selection

- Define evaluation criteria
- Perform technical and economic parametric analyses of the potential design improvements to the baseline RS
- Select concept.

Task 4--RS Design and Analysis

- Prepare Design Analysis Plan
- Analyze receiver operation and define auxiliary equipment required
- Perform thermal/hydraulic (T/H), structural, mechanical, and control design and analysis, and efficiency analysis.

Task 5--RS Cost and Fabrication Plans

- Develop shop fabrication and field construction plans
- Estimate RS cost.

Task 6--Receiver Fabrication Process Development

- Prepare detailed Fabrication Process Development Plan
- Develop techniques for tube-to-tube and tube-to-header joining and methods for attaching panels or panel tubes to support structure
- Evaluate techniques with mechanical tests
- Perform stress analysis to evaluate the effect of stresses and strains arising from the joining and attaching methods.

Task 7--Subsystem Research Experiment and Development Plan

- Identify Subsystem Research Experiment (SRE) requirements
- Prepare SRE design, plan, and schedule.

Task 8--Phase 2 Plan and Proposal (deleted)

- Prepare detailed proposal for continuing effort into Phase 2.

Task 9--Reports and Data

- Prepare and submit reports and data as specified by SNLL
- Attend contract meetings.

Task 10--Program Management

- Coordinate and direct project effort
- Establish budgets and control costs
- Conduct independent technical and design reviews
- Monitor technical progress
- Interface with the SNLL Technical Contract Manager.

1.1.5 Project Team

To perform the Phase 1 design study, we assembled a team of organizations with valuable complementary backgrounds in systems and design integration; design, fabrication, construction, and testing of central receiver solar thermal power systems and components; and operation of utility generating plants. Foster Wheeler Solar Development Corporation (FWSDC), prime contractor for Phase 1, had overall responsibility for the project. The team consisted of our affiliated companies--Foster Wheeler Energy Corporation (FWEC) and Foster Wheeler Special Projects Engineering and Construction, Inc. (FWSPEC); McDonnell Douglas Corporation (MDC); Arizona Public Service Company (APS); Sierra Pacific Power Company (SPP); and Olin Corporation. Table 1.1 shows the team members and their primary areas of responsibility.

Table 1.1 Team Responsibilities

| <u>Organization</u> | <u>Responsibility</u> |
|---------------------|--|
| FWSDC | Overall project management and coordination, receiver design and analysis, fabrication process development, SRE conceptual design |
| FWEC | Fabrication plan and cost estimates, receiver mechanical design |
| FWSPEC | Design of receiver tower and piping system, specification of salt pump and auxiliary equipment, construction plan and cost estimates |
| MDC | Development of system-level requirements and specifications, selection of preferred receiver configuration, definition of incident fluxes, performance estimates, control system, SRE plan |
| APS, SPP | Provide utility engineering review |
| Olin | Molten salt technology advisor. |

1.2 SELECTION OF THE RS1.2.1 Trade-Off Studies

Absorber configuration trade-off studies included parametric analyses of:

- Absorber surface arrangement, including tilted vs. vertical orientation
- Absorber materials
- Tube dimensions
- Allowable flux levels
- T/H stability
- Panel geometry, arrangement, and flow routing

Other trade-offs that were made in parallel include:

- Aperture door configuration and size
- Overnight conditioning
- Feed pump arrangement
- Receiver protection

The output of these analyses was used to complete the definition of the RS equipment, cost, and performance and to provide data for the final configuration selection. For those configurations that were most attractive, we estimated receiver losses, rescaled the collector field and tower configurations, and calculated annual energy delivered to thermal storage.

We defined the auxiliary equipment required for overnight conditioning, start-up, shutdown, and emergency operation. In these analyses we investigated options for keeping the panels hot overnight as opposed to draining them overnight and preheating them before early morning start-up. The requirements for overnight heating were assessed and the trade-offs between electrical trace and

radiant heating of the panels and the circulation of heated salt were investigated. We compared the fill and drain of the downcomer with overnight hold. In all of these cases, we addressed both equipment costs and parasitic power requirements. Surge tanks and selected pumping or pressurizing schemes were sized to provide emergency coolant flow in the event of a power or receiver feed-pump failure. We also identified options for the aperture door.

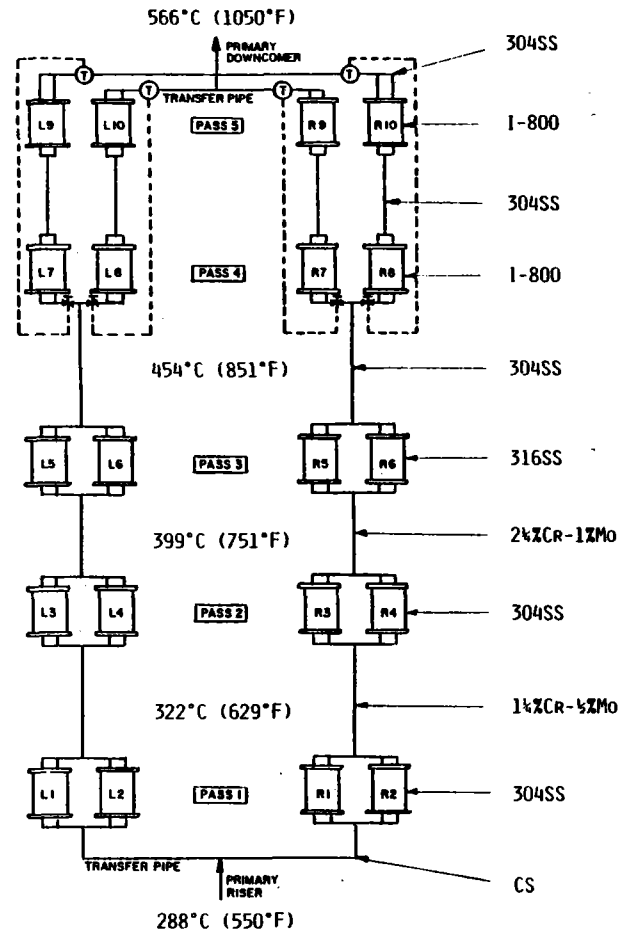
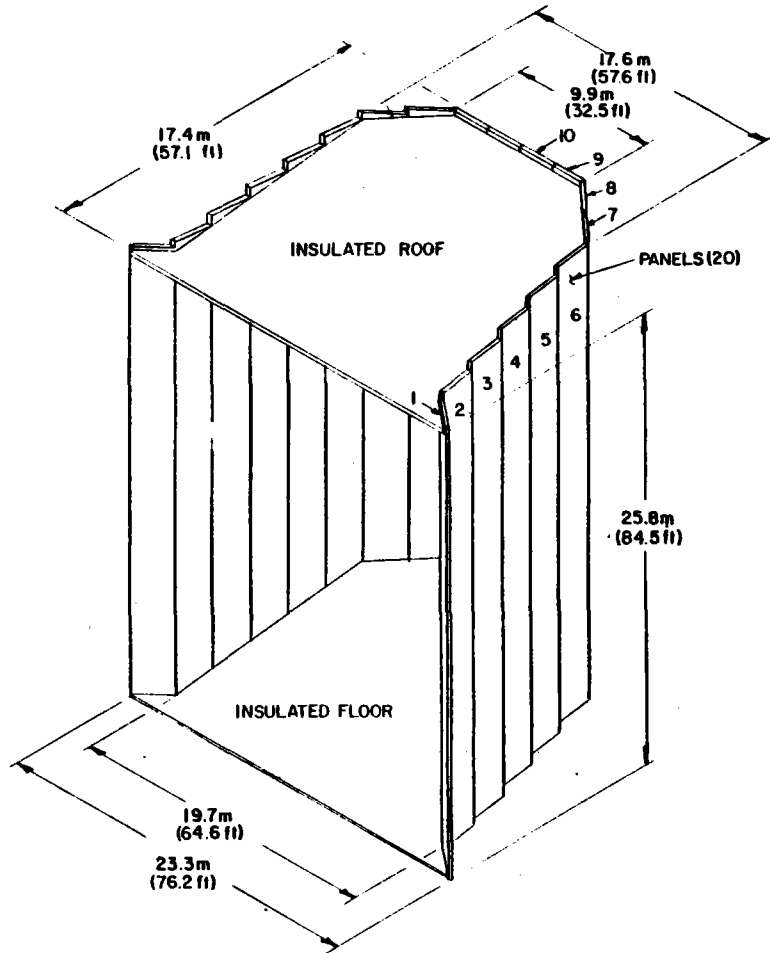
Dominant factors in the initial screening of absorber configurations were minimum area consistent with peak heat flux, with heat flux levels near the outlet where high salt film (I.D.) temperatures occur, and with heat flux gradients across the panels. Tube characteristics were selected to satisfy a combination of high-temperature thermal structural (i.e., peak heat flux) capabilities, ease of fabrication, and low cost. Flow routing was selected primarily because of the need for low heat flux in the high-temperature panels and to ensure a low pumping power requirement and good T/H stability over a wide load range. The selected absorber configuration ultimately embodied all these factors.

At SNLL's request, we investigated overnight drain and either preheat with the aperture door closed or preheat with heliostats (no door required) before fill and start-up. The analysis indicated that, by utilizing the heliostat field to preheat the panels, a start-up delay of 19 minutes and thus a loss of 1.3 percent of the annual collected energy would result, compared with a saving of 0.7 percent in auxiliary electricity if the receiver were not heated overnight. The major impact on annual energy will be caused by time lost from

either door problems in the heated case or fill problems in the unheated case. While door reliability/availability has not been assessed, the panel preheat analysis has shown that substantial differences in panel temperatures are likely for a partial cavity configuration and that a slow and careful heat-up will be required to preheat the panels in a safe manner. The complexity of this procedure is such that its application to commercial practice is questionable. In addition, some fraction of operating time beyond initial morning hours may be lost as a result of inability to fill. Final resolution of this trade-off study appears to depend on the reliability and cost of the aperture door. In this study we decided to use the door/no-drain/heated option and proceed with the effort to generate a detailed door design and cost estimate. These data, along with door reliability data from Phase 2, will be used to reevaluate this trade-off for future commercial receiver designs.

1.2.2 Selected Configuration

The cavity configuration was selected primarily to minimize thermal losses during operation and overnight or cloudy-day shutdown. It is a partial cavity absorber with 20 vertical up-flow panels (Figure 1.2). This arrangement combines high performance with low-cost fabrication and construction based on modular replaceable panels. There are 18 internal panels and two semi-external "wing" panels--one on each side of the aperture at an angle of 45 deg to the aperture plane. Because they are low-temperature panels, the wing panels reduce spillover without major increases in losses.



11-1

Figure 1.2 Absorber Isometric and Circuitry

The receiver feed pump arrangement--three half-capacity pumps (two operational and one spare)--was chosen on the basis of reliability and to minimize auxiliary power--especially at the low loads common during early morning and evening operation.

Primary requirements for the door include good sealing to minimize heat loss through air convection, rapid closing (by gravity) to protect the absorber in the event of loss of salt flow and the inability to defocus the heliostat field because of either power or control system failures, and ability to withstand incident flux in the closed position without permanent damage. We selected a fast-closing two-section door that could close either mechanically or by gravity.

The criteria most important in the evaluation of the overnight conditioning approach were cost, reliability, ease of installation, and maintenance. The selected approach utilizes an aperture door with double seals, radiant cavity heaters, trace heating of all salt piping, and thermal energy from the Outlet Surge Tank (OST). Radiant heaters were selected because of operating simplicity, low capital cost, and inherent redundancy in the modularity of the units. This approach was selected because it offers the greatest flexibility, provides for morning start-up without heliostat preheat of the panels, and provides for receiver protection in the event of a power failure, using the aperture door.

Receiver protection included considerations of redundancy, use of proven components, and cost. Features include 1 minute of emergency salt flow from the

pressurized Inlet Surge Tank (IST), rapid heliostat field defocus, diesel generator backup power, aperture door with sacrificial ablator on the outside, and three half-capacity pumps that will permit operation to continue if one pump fails.

The most serious failure is the loss of salt flow to the absorber panels under solar incident flux, which could result in tube failure, warping, or reduction in panel life. In this case, the heliostats must be defocused from the receiver while the emergency flow supply from the IST maintains some coolant flow. As long as the collector field can operate, such an approach is adequate; however, if the heliostats cannot be defocused because of either power or control system failures, the length of time required for the earth to rotate to reduce incident fluxes is too long to prevent damage to the absorber panels. Protection during this combination failure is provided by the quick-closing door with ablative face and emergency salt flow from the pressurized IST.

A concrete tower was selected because of its lower capital and maintenance costs.

1.2.3 Materials Selection

The material for the absorber panels and headers was selected after a review of high-temperature mechanical properties and a number of SNLL's corrosion testing programs. These tests determined the degrees of susceptibility of various alloys to general corrosion and stress corrosion in a molten salt environment.

Uncertainty regarding creep-fatigue data exists not only for molten salt receivers but for all types of solar receivers. Lack of appropriate data will create uncertainty in the life of the receiver components, especially the absorber panels. Extensive creep-fatigue tests with hold times of 1 to 6 minutes on tubes of various materials in a molten salt loop are recommended. However, while these tests would be very useful in the long term, data would not be generated in time to meet the schedule for this program. In our opinion, the best alternative would be to design the receiver so that panels or individual tubes can be replaced easily and to accept the fact that tube life in certain critical, high-temperature zones in the receiver might be less than the desired design life.

In view of these considerations and to meet the 30-year design life requirement, Incoloy 800 material was selected for the high-temperature absorber panels. The Incoloy 800 was selected over the austenitic stainless steels because it is much stronger at elevated temperatures and has good low-cycle fatigue strength and ductility. Type 316SS could have been used in the high-temperature panels, but our analysis indicated that it would not meet the 30-year design life. For the low- and medium-temperature panels, Types 304SS and 316SS alloys were selected.

For panel modularity, which would minimize the number of spares required by the utility, one option was to have all absorber panels made of Incoloy 800. The other option was to have identical panels made of different materials: Types 304SS and 316SS and Incoloy 800 for the low-, medium-, and high-temperature panels respectively. Because the "all-Incoloy 800"

option imposes a very high cost penalty, we selected the "multiple materials" option--panels identical in all respects but materials. Thus the utility can still have a minimum number of spares made of Incoloy 800 to use as a replacement for any receiver panel.

As shown in Figure 1.2 the panel tubes are Type 304SS for Passes 1 and 2, Type 316SS for Pass 3, and Incoloy 800 for Passes 4 and 5. The inlet transfer pipe, primary riser, and cold surge tank are carbon steel. The outlet transfer pipe, primary downcomer and hot surge tank are Type 304SS. Downcomers between passes are 1-1/4%Cr-1/2%Mo for Pass 1, 2-1/4%Cr-1%Mo for Pass 2, and Type 304SS for Passes 3 and 4.

1.3 RS DESIGN ANALYSIS

The conditions to which the molten salt RS is designed are defined in the RS Requirements Specification, which was prepared based on the requirements in the revised specification from Task 1, the data obtained in the literature review, and the experience of the team members. It was updated at the end of Task 3 and was compiled in final form at the end of Task 4. The document defines the following:

- RS scope
- Applicable codes and standards
- Technical requirements
- Interface requirements
- Environmental requirements.

The design conditions are summarized in Table 1.2.

1.3.1 Design Point

Since the best collector field performance occurs at or near noon on February 19 (day 50 in DELSOL numbering), we selected this time as the design point. Maximum performance on February 19 rather than winter solstice (best field cosine time) results from decreased shadowing and blocking losses, which more than compensate for the reduction in field cosine.

RS operation without defocus was limited to 1000 W/m^2 ($317 \text{ Btu/h}\cdot\text{ft}^2$). This limit results from analysis of 4 years of detailed direct normal insolation data for Barstow. These data show that, on the average, only 12.5 percent of the days have insolation above 1000 W/m^2 ($317 \text{ Btu/h}\cdot\text{ft}^2$), whereas over

Table 1.2 RS Design Data Summary

| | |
|--|--|
| Reference site | Barstow, California |
| Configuration | Partial cavity. Replaceable modular panels (20). All up-flow panels. Gravity-closing aperture door. |
| Aperture midpoint elevation | 216 ±1.0 m (709 ±3.3 ft) |
| Heat-transfer fluid | Molten nitrate salt |
| Service life | 30 years |
| Availability and reliability | 0.95, exclusive of insolation |
| Maximum transportation length | 35 m (115 ft) |
| Design point | Noon, February 19 (Day 50) |
| Design point insolation | 950 W/m ² (301 Btu/h·ft ²) |
| Maximum insolation | 1000 W/m ² (317 Btu/h·ft ²) |
| Absorbed power | 320 MW (1092 x 10 ⁶ Btu/h) |
| Minimum absorbed power at rated conditions | 80 MW (273 x 10 ⁶ Btu/h) |
| Maximum incident flux | 0.65 MW/m ² (0.206 x 10 ⁶ Btu/h·ft ²) |
| Salt flow rate | 760 kg/s (6.018 x 10 ⁶ lb/h) |
| Salt inlet/outlet temperature | 288/566°C (550/1050°F) |
| Overnight salt temperature | 288°C (550°F) |

50 percent of the days have insolation above 950 W/m^2 ($301 \text{ Btu/h}\cdot\text{ft}^2$), and none have insolation greater than 1069 W/m^2 ($339 \text{ Btu/h}\cdot\text{ft}^2$).

Results of a preliminary trade-off between the energy gained by increasing receiver size to accept higher powers and additional annual energy and the energy lost from increases in receiver losses because of its larger size indicated that the trade-off is very close between 950 and 1000 W/m^2 (301 and $317 \text{ Btu/h}\cdot\text{ft}^2$). Because of the potential for operating errors and the reliability of measured insolation, 950 W/m^2 ($301 \text{ Btu/h}\cdot\text{ft}^2$) was chosen as the design point for a first-of-a-kind plant.

As a design margin, peak tubewall temperatures for stress analysis were also calculated at the maximum insolation conditions-- 1000 W/m^2 ($317 \text{ Btu/h}\cdot\text{ft}^2$).

1.3.2 Thermal/Hydraulic Design Analysis

The major T/H design analysis tasks were:

- Steady state
- Transient
- Thermal conditioning
- Performance

The T/H analysis was based on the revised molten salt properties received from SNLL during Task 3. At the design point heat flux, receiver power output is 320.04 MW ($1092.04 \times 10^6 \text{ Btu/h}$). Performance calculations show that the required receiver output to meet the RS rated power of 320 MW ($1091.88 \times 10^6 \text{ Btu/h}$) is 318.3 MW ($1086.08 \times 10^6 \text{ Btu/h}$); the difference is made up by 1.7 MW ($5.8 \times 10^6 \text{ Btu/h}$) of viscous dissipation in the downcomer and drag valve.

The maximum absorbed heat flux and peak front-to-back tube ΔT --0.614 MW/m² (195 x 10³ Btu/h·ft²) and 153°C (275°F) respectively--occur in the center tube of Panel 4, Pass 2. The peak tubewall (O.D.) and salt film (I.D.) temperatures--633°C (1171°F) and 601°C (1114°F) respectively--occur in the left tube of Panel 9, Pass 5 (Figure 1.3). At this location the absorbed peak heat flux is 0.381 MW/m² (121 x 10³ Btu/h·ft²). Thus the recommended maximum salt film (I.D.) temperature--593°C (1100°F)--is exceeded in Pass 5.

At the point of maximum salt film (I.D.) temperature, the salt bulk temperature is 554°C (1029°F), which results in a salt ΔT (I.D. temperature minus bulk temperature) of $\approx 47^\circ\text{C}$ ($\approx 84^\circ\text{F}$). To meet the recommended maximum, we will

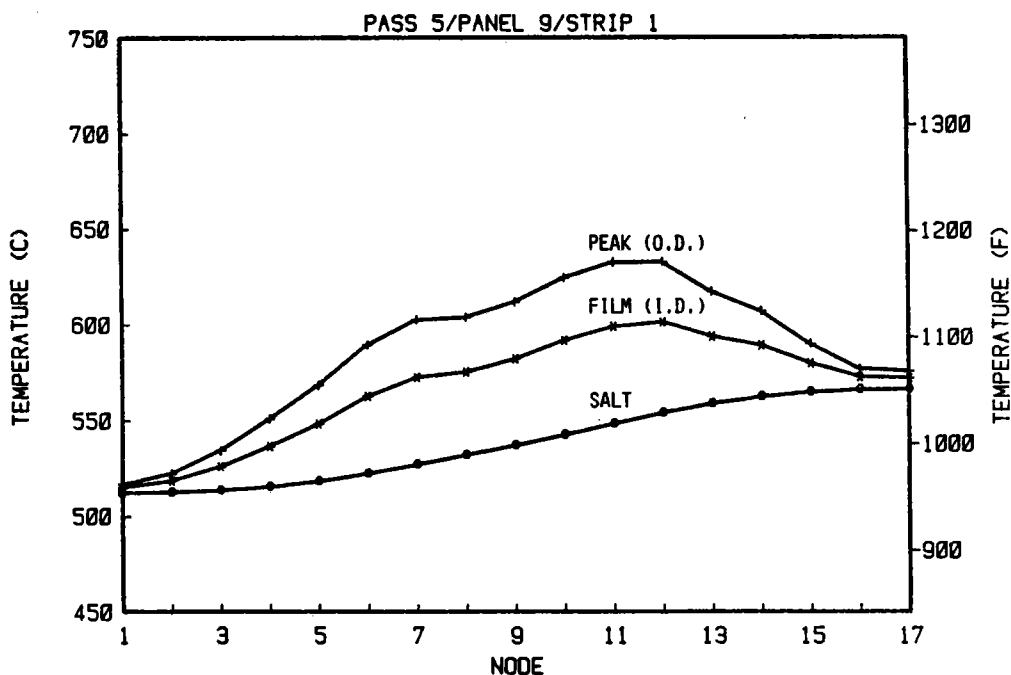


Figure 1.3 Temperature Profile of Absorber Hottest Tube

have to reduce the heat flux at this location by about 17 percent--a reduction that could be difficult to achieve within acceptable cost limits.

Experimental programs at Olin show that some alternatives exist that should solve the salt decomposition problem, such as physically adding nitrates or oxidizing the nitrites to nitrates to restore the original salt composition. These molten salt stabilizer research methods have been demonstrated by Olin under laboratory test conditions, but further testing is required under conditions at pilot plant scale.

The quantity of salt exposed to this temperature is only a small fraction of the total salt flow rate, and it is exposed for only a short period of time because of the velocity of salt through the tubing [about 3 m/s (10.1 ft/s) in the outlet panels] and the resultant turbulent mixing. As a solution, we recommend that the required salt outlet temperature be reduced by 14°C (25°F) to 552°C (1025°F) for the first commercial plant, unless methods to make the salt fully compatible with the higher temperature limit have been fully demonstrated by that time.

The sensitivity of salt flow and of salt outlet and tubewall temperatures to variations in heat flux across the panels was investigated at full- and part-load conditions at the design point. The results indicate that changes in salt flow rate and outlet temperatures for the worst variation in heat absorption (Pass 1) are not significant at or near full load. The coldest tube within that pass has approximately 1.8 percent less flow than the average tube. Consequently, salt flow through the panel tubes is very insensitive to heat flux

variations across the panel width, and each tube within a given panel has essentially the same salt flow rate. This is not the case for 10-percent flow, where the assumption of equal flow per tube is no longer valid. Because of this and the possibility of being in the transition region, we do not recommend operation with less than 25-percent full flow. From 0 to 25 percent is considered start-up.

The RS performance was calculated for both annual average operating conditions and design point conditions. The receiver was analyzed for spillover, reflection, reradiation, convection, and conduction losses; using the results of these analyses, the RS efficiency was calculated. Table 1.3 summarizes the design point and annual average losses/efficiency for the RS.

Table 1.3 RS Performance

| | <u>Design Point (MW)</u> | <u>Annual Average (10³ MWh)</u> |
|----------------------------------|------------------------------|--|
| Incident power at aperture plane | 363.3 | 849 |
| Spillover | -14.7 | -34 |
| Reflection | - 6.4 | -14 |
| Reradiation | -10.0 | -32.1 |
| Convection | -13.6 | -42.9 |
| Conduction | - 0.3 | - 2.6 |
| Viscous dissipation | <u>+ 1.7</u> | <u>+ 4.0</u> |
| RS output power at base of tower | 320.0 | 727.4 |
| RS overall efficiency | 0.88 | 0.86 |

The RS heat loss rate during overnight shutdown with the electric radiant and trace heaters maintaining the salt at 287.8°C (550°F) was calculated as ≈ 560 kW (1.91×10^6 Btu/h) at the design point ambient temperature and wind speed.

Table 1.4 summarizes the T/H data.

1.3.3 Stress Analyses

Those sections of the receiver subjected to radiant heating (i.e., the absorber panels) are the most critical component from the thermal-stress and creep-fatigue points of view. Hence we analyzed the panels extensively to determine the severity of the thermal stresses and their impact on the structural integrity and creep-fatigue life of the receiver.

In the design of the pressure boundary, all requirements of the ASME Boiler and Pressure Vessel Code, Section VIII-Division 1 were satisfied. In addition, because of the highly cyclic nature of receiver operations, the fatigue criteria of Section VIII-Division 2 for temperatures in the sub-creep regime were satisfied. For elevated temperature design, we analyzed for creep-fatigue based on the linear damage addition approach of Code Case N-47. Strict adherence to Code Case N-47, however, is too conservative for solar applications and will result in severe economic penalties. Hence the approach in Code Case N-47 was used with some modifications. One modification that we have proposed for use with solar applications is the use of inelastic fatigue curves (Figure T-1420-1C of Code Case N-47) in conjunction with inelastic strains approximated from an elastic analysis.

Table 1.4 Thermal/Hydraulic Performance Data Summary

| | |
|---|---|
| Heat-transfer fluid | Molten nitrate salt |
| Maximum absorbed power | 336.8 MW (1149.3 x 10 ⁶ Btu/h) |
| Nominal absorbed power | 320.0 MW (1092.0 x 10 ⁶ Btu/h) |
| Peak absorbed heat flux | 0.614 MW/m ² (195 x 10 ³ Btu/h•ft ²) |
| Average absorbed heat flux | 0.254 MW/m ² (81 x 10 ³ Btu/h•ft ²) |
| Design point RS efficiency | 0.881 |
| Annual average RS efficiency | 0.859 |
| Peak tubewall (O.D.) temperature | 633°C (1171°F) |
| Peak salt film (I.D.) temperature | 601°C (1114°F) |
| Peak front-to-back tube ΔT | 153°C (275°F) |
| Salt flow rate | 760 kg/s (6.018 x 10 ⁶ lb/h) |
| Salt inlet/outlet temperature | 288/566°C (550/1050°F) |
| Salt Reynolds number, minimum to maximum | 34,800 to 114,700 |
| Salt velocity, minimum to maximum | 3.0 to 3.4 m/s (9.7 to 11.2 ft/s) |
| Salt film coefficient, minimum to maximum | 5780 to 10,250 W/m ² •°C (1020 to 1800 Btu/h•ft ² •°F) |
| Receiver frictional Δp | 1517 kPa (220 lb/in ²) |
| Feed pump inlet pressure | 345 kPa (50 lb/in ² g) |
| Feed pump outlet pressure | 6895 kPa (1000 lb/in ² g) |
| Inlet surge tank operating pressure | 2410 kPa (350 lb/in ² g) |
| Outlet surge tank operating pressure | 103 kPa (15 lb/in ² g) |

We estimated the creep-rupture life using the rupture life curves of Code Case N-47. However, only the pressure stresses (as opposed to thermal plus pressure stresses as recommended in Code Case N-47) were used in evaluating the rupture life. We added the creep and fatigue damage fractions and limited this value to 1. This analysis showed the receiver life requirements were satisfied for diurnal and cloud cyclic operation.

With regard to material properties, both Types 304SS and 316SS are qualified materials under the Code, and their creep and fatigue properties are well documented. Although Incoloy 800 is an accepted Code material, the Code does not list its creep and fatigue data. However, the Code has rupture life and allowable cycles graphs for Incoloy 800H. Because the material properties are very similar for Incoloy 800 and 800H at the absorber panel design temperatures, the creep-fatigue data for 800H were used.

Transient temperature distribution and stress analyses were done for the receiver panels for several start-up and shutdown transient conditions. Essentially, five transients were evaluated:

- Morning hot start-up
- Noon hot start-up
- Hot shutdown
- Emergency shutdown
- Cloud-cover

Of the three locations chosen for creep-fatigue evaluation (Pass 2--Type 304SS, Pass 3--Type 316SS, and Pass 4--Incoloy 800), we selected Pass 2 and Pass 4 for transient analysis. We did not perform the analysis for Pass 3 because the

effect of transient stresses is primarily on fatigue, and Pass 2 fatigue conditions are more severe than those in Pass 3. [The fatigue properties of Type 304SS (Pass 2) and Type 316SS (Pass 3) are identical.]

At no time during the transient event do the tubewall temperatures and ΔT s--and thus the stresses--exceed the corresponding steady-state values.

1.3.4 Mechanical Design Analysis

The major mechanical design tasks were:

- Absorber panels
- Surge tanks and interconnecting piping
- Absorber door
- Receiver structure
- Tower and tower foundation
- Riser and downcomer piping

Component-level drawings were prepared in sufficient detail to allow preparation of RS fabrication and construction/erection plans and cost estimates.

The RS mechanical design was performed in accordance with the RS Requirement Specification. All pressure parts were designed in accordance with the ASME Boiler and Pressure Vessel Code. The structural analysis complies with all the requirements of the Uniform Building Code (UBC), the American Institute of Steel Construction (AISC), and all other applicable codes and standards.

The design salt flow rate was used to size the riser/downcomer pipes. It is a conservative assumption, since the average salt flow rate will be less than the design value. The primary riser was sized to minimize combined costs for both pumping and piping. The optimum riser size was determined as 0.41 m

(16 in.) O.D. Since pumping costs are independent of downcomer size, the downcomer was sized to dissipate a large percentage of the gravity head at the design flow rate. A 0.30 m (12 in.) O.D. was selected; it will dissipate \approx 75 percent of the gravity head by friction. The remainder is dissipated by the drag valve and the field return piping to the Storage Subsystem.

Piping materials were selected based on results of the material selection work. The carbon steel riser carries cold salt at 288°C (550°F). The Type 304SS downcomer carries hot salt at 566°C (1050°F). Piping wall thickness was calculated in accordance with the American National Standards Institute (ANSI) B31.1 Power Piping Code. Insulation thickness was chosen from Foster Wheeler design manuals.

1.3.5 Operation and Control Analysis

Six major operating modes were identified--cold drained, hot drained, hot standby, derated operation, rated operation, and overnight standby--and the transitions between these modes were developed. These transitions are:

- Cold drained to hot drained
- Hot drained to hot standby
- Hot standby to derated operation
- Derated to rated operation
- Overnight standby to hot standby
- Rated operation to derated operation
- Derated operation to hot standby
- Hot standby to overnight standby
- Overnight standby to hot drained
- Hot drained to cold drained

The operating procedures for the RS were specified to aid in the design and selection of the RS control system.

The control system response was analyzed in three sequential stages. The controller was modeled using a state variable representation of an analog controller. During this stage only a 10-percent cloud variation was modeled using back tubewall temperatures for feed-forward information. Subsequent to this analysis, the controller models used in the simulation were updated to represent more accurately the type of controller proposed for the RS. The new controller model simulates a Beckman controller with simple derivative filtering. Using this updated controller model, we addressed both a 10- and a 50-percent cloud and considered both back tubewall temperatures and flux gages for feed-forward information. Because the results were preliminary, a final analysis of a 50-percent cloud was performed.

The results indicate that 50-percent step changes in power level will produce transient temperature variations of approximately $+10/-15^{\circ}\text{C}$ ($+18/-27^{\circ}\text{F}$) damping down to $\pm 3^{\circ}\text{C}$ ($\pm 5.4^{\circ}\text{F}$) in approximately 150 seconds. The flux gage data showed a slight advantage [$\approx 3^{\circ}\text{C}$ ($\approx 5.4^{\circ}\text{F}$) less undershoot in temperature]. Both systems appear promising based on the simulation results. Actual test data will be essential to validate the simulation models for the key physical processes and the simulation results.

1.4 RS SUMMARY DESCRIPTION

The receiver is located south of the heliostat field, atop a reinforced concrete tower. Figure 1.4 shows the front and back views of the receiver; configuration data are summarized in Table 1.5.

The right and left sides of the absorber are symmetrical, mirror images. The panels on each side form two independent parallel-flow circuits. Each circuit comprises 10 panels connected into five passes (Figure 1.2). Upward flow in the panels minimizes the possibility of T/H instability. Four control valves (two per side) maintain the desired outlet temperature by controlling both the amount and distribution of salt flow.

The absorber panels are fabricated in individual modules or subassemblies to facilitate handling during fabrication, shipment, and erection. Panel configuration is basically very similar to that of a typical, conventional utility boiler panel. The panels are made of 88 tubes continuously welded to adjacent tubes with spacer strips to form three solid subpanel sections 28, 32, and 28 tubes wide. Each subassembly--consisting of the panel tubes, inlet and outlet headers, buckstays, support struts, and strongbacks--is shop-built and shipped as a unit. Insulation and sheathing are added during erection. Including insulation, the gross weight of an entire subassembly is 10,900 kg (24,000 lb).

Key features of the absorber panel are:

- Modular shop assembly simplifies transportation, erection, and replacement.
- All panels are identical except for tube/header materials and insulation thickness.

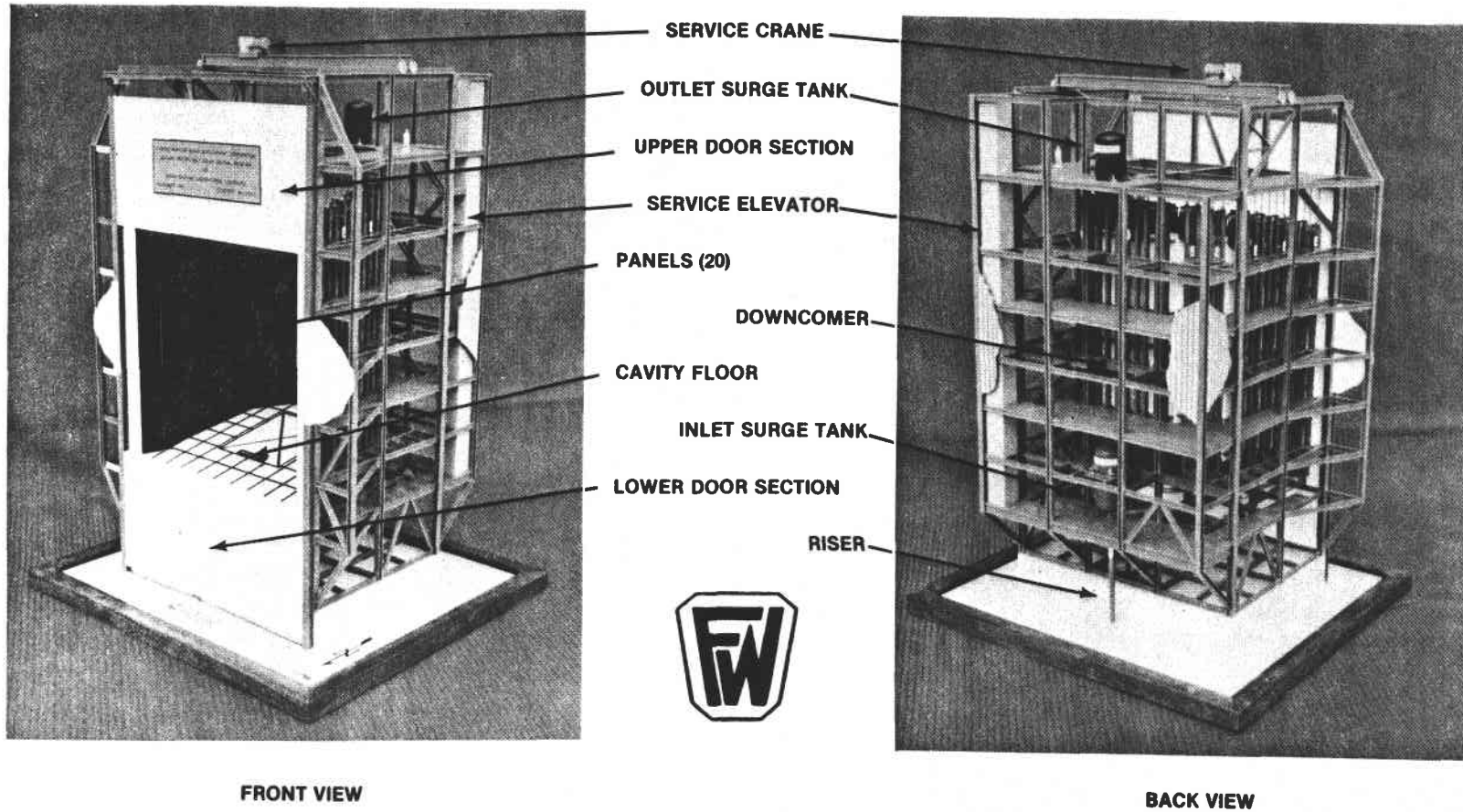


Figure 1.4 320-MW Molten Salt Solar Cavity Receiver

Table 1.5 Configuration Data Summary

Receiver

| | |
|--|---|
| Overall [height x depth (N-S) x width (E-W)] | 55.2 x 25.6 x 32.0 m (181 x 84 x 105 ft) |
| Cavity (width x height x depth) | 19.8 x 25.8 x 17.4 m (65 x 84.5 x 57 ft) |
| Aperture (width x height) | 19.8 x 25.8 m (65 x 84.5 ft) |
| Aperture area | 510.2 m ² (5492 ft ²) |
| Total frontal area including wing panel | 592.2 m ² (6375 ft ²) |
| Total exposed (active) area | 1258 m ² (13,542 ft ²) |
| Total wet weight | 1341 x 10 ³ kg (2950 x 10 ³ lb) |

Absorber Panels

| | |
|-------------------------------------|---|
| Construction type | Continuously welded tubes with a spacer strip between |
| Tube material | 304SS/316SS/Incoloy 800 |
| Number of panels | 20 |
| Number of tubes per panel | 88 |
| Overall length x width | 28.4 x 2.44 m (93.4 x 8.01 ft) |
| Distance between header centerlines | 27.5 m (90.25 ft) |
| Exposed (active) length | 25.8 m (84.5 ft) |
| Exposed (active) surface | 62.9 m ² (677.1 ft ²) |
| Tube O.D. x wall thickness | 25.4 x 1.65 mm (1.0 x 0.065 in.) |
| Spacer strips, thickness x depth | 2.381 x 11.1 mm (3/32 x 7/16 in.) |
| Design pressure | 3463 kPa (350 lb/in ² g) |
| Panel weight (empty) | 10,000 kg (24,000 lb) |

- Swing links eliminate frictional restraint of expansion, but provide excellent strength.
- Vertical splits in panel reduce forces required to keep panel straight and in plane.
- Horizontal expansion is controlled by limit stops between buckstays and tube lugs.
- Jumper tubes permit differential thermal expansion.

The cavity floor and ceiling are uncooled surfaces consisting of Fiberfrax Duraboard weatherproof insulation anchored to carbon steel plate. The floor supports radiant heaters for absorber thermal conditioning to prevent salt from freezing during shutdown. The floor and ceiling are made of sections that can be lifted out by an overhead crane. Flexible seals between the floor and absorber panels minimize thermal losses from the cavity.

A skeletal structure supports the absorber and associated equipment. There are two major platform levels (one at the top and one at the bottom) and two intermediate levels. The height of the structure was determined by the travel of the upper door section. A bridge crane runway and machine room for the elevator are located at the top level of the structure (Figure 1.4).

Key features of the receiver structure are:

- Four major support columns that comprise part of the four major braced bents
- Bent arrangement that minimizes torsional loading on rear of structure
- No obstruction to lifting and positioning of panel modules
- A service crane to complete receiver installation when basic structure is erected.

One of the major advantages of our design is the ability to remove complete panel modules for maintenance. The 15-ton overhead crane can travel across the receiver, remove sections of the roof and floor, pick up any panel/strongback module, and lower it through the center of the receiver and tower to the ground. The overhead crane can also be used during construction, as soon as the structure is erected. During receiver operation the crane will be stored in the rear of the structure, away from the hot air coming from the cavity aperture.

The aperture door is a two-section guillotine-type with a hollow core for heat dissipation within the door structure to prevent it from warping. It minimizes thermal losses when the receiver is not in operation and protects the receiver in the event of feed pump or power failure. Each section of the door spans the receiver aperture horizontally. When the door is opened and closed by a cable drum-type hoist mechanism, the sections move up and down parallel to the receiver aperture on vertical tracks. The lower section counterbalances the upper section, minimizing the power required for opening and closing it. The two sections are similar in construction, but the upper section is larger and heavier to permit closing by gravity in the event of a power failure. The aperture side of the door is faced with a layer of Fiberfrax blanket insulation. The front side is protected by a layer of ablative material to protect the door (and the absorber) during an emergency until the motion of the earth moves the incident solar flux away from the receiver or the heliostats are otherwise defocused.

Key features of the door are:

- Fabricated truss plus corrugated sheet surface give light and rigid door.
- Maximum free area through door structure assists convective cooling of door.

- Four-point spherical bearing attachment to trolleys eliminates binding as a result of distortion.
- Double seal minimizes convection losses when receiver is "bottled up."
- Short and direct load path exists from door rails to structural steel.
- Operation is simple and reliable compared with multiple-section or "up and over" doors.

The receiver tower is a slip-formed, reinforced-concrete structure rising 193.7 m (635.5 ft) above ground level. The tower contains an internal elevator, lightning protection equipment, aircraft warning lights, and receiver auxiliary machinery. The primary salt riser and downcomer are supported along the inside of the tower shell with expansion loops at appropriate intervals.

The energy transport loop consists of the primary riser, the primary downcomer, IST, OST, the receiver feed pumps, valves, and associated instrumentation. All energy transport loop equipment is fully drainable, heat traced, and insulated.

Figure 1.5 illustrates the overall flow schematic. Cold salt at 288°C (550°F) is pumped from the Cold Storage Tank (CST) through the field supply piping and tower riser to the receiver. At the inlet to the receiver, the salt flow is divided in two, one stream for each half of the absorber. Each proceeds through 10 panels in both series and parallel paths, heating in the process to 566°C (1050°F). The hot salt then flows by gravity through the tower downcomer, drag control valve, and field return piping to the Hot Storage Tank (HST). Downcomers are provided after each pass through a panel or set of panels so that all panels have upward flow. Separate control valves

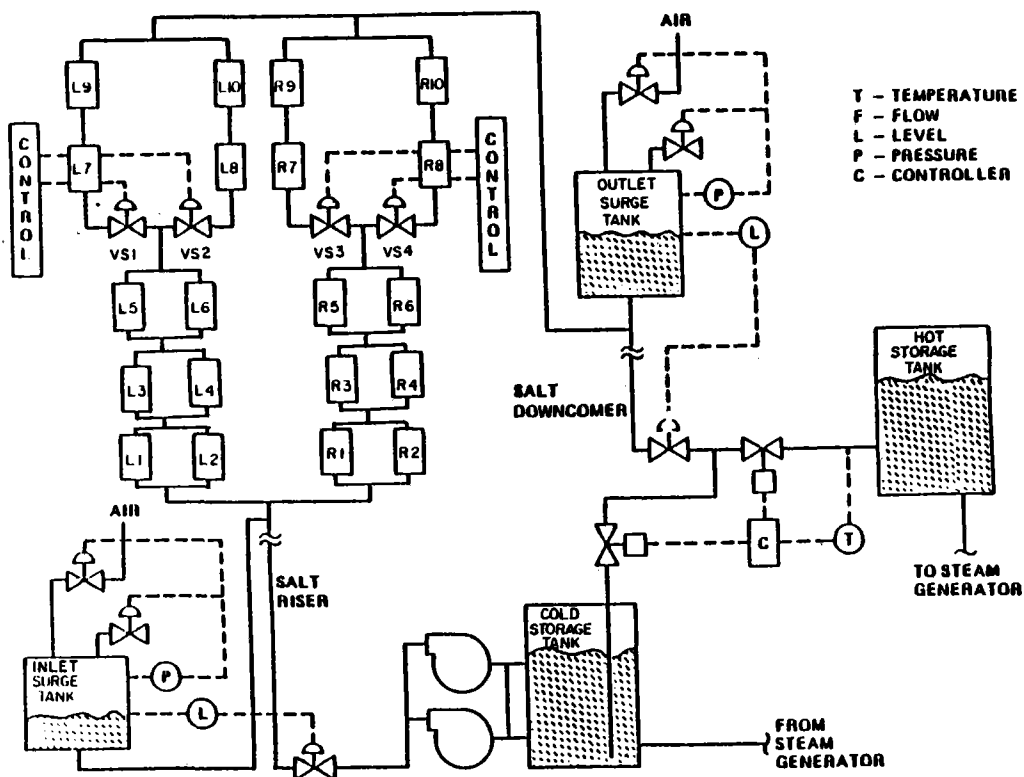


Figure 1.5 RS Flow Schematic

downstream of Pass 3 control the outlet temperatures of Passes 4 and 5 by distributing the flow in proportion to the absorbed power. In addition to outlet temperature data, flow control uses feed-forward information on input power changes (either flux gage data or temperature data) to anticipate rapid flow changes required during partly cloudy conditions.

Figure 1.5 also illustrates the relationship of the surge tanks to the receiver circuitry. The IST and OST atop the tower buffer the faster acting control valves from the slower responding salt pump and drag control valves. Level sensors on these tanks control the feed pump recirculation valve and the

drag valve at the bottom of the downcomer. Tank levels are set at one-half to provide a control margin and a ready supply of salt. The pressurized IST provides an emergency salt flow to protect the receiver in case of feed pump or power failure. The OST connected to the primary downcomer is located above the highest absorber panel header for positive filling of the absorber panels and piping. Compressed air for the surge tanks is supplied by an air compressor and storage tank located at the base of the tower.

1.5 PANEL FABRICATION DEVELOPMENT

Welding development was undertaken to resolve fabrication issues and to develop basic methods for continuous longitudinal welding of thin-walled tubes to form flat panels and for attachment of support lugs to the panels.

A semiautomatic short-circuiting arc (dip transfer) metal inert gas (MIG) welding process was chosen for longitudinally welding tubes to form a panel. This process was chosen because of its ability to produce sound welds in thin sections with minimal tubewall penetration.

A MIG welding head (Figure 1.6) was designed and fabricated to feed a consumable bare electrode into the weld zone at a constant rate and supply a continuous blanket of inert gas to shield the weld zone from atmospheric contamination. As shown in the figure, the welding head was mounted on a horizontal cross-beam carriage. A drive mechanism moved the head along the carriage at a constant, predetermined rate.

For trial welding, we bolted a series of scalloped support blocks to a rigid, flat table. These blocks supported three tubes on the table at 0.15-m (6-in.) intervals. Pneumatically activated toggle clamps (also shown in the figure) held the tubes firmly on the support blocks and prevented them from moving during welding. The clamps were automatically activated to open at each clamp site as the welding head traversed the length of the tubes.

Several trial welds were made to determine the best tube-to-tube longitudinal weld configuration. They indicated the need for a spacer strip.

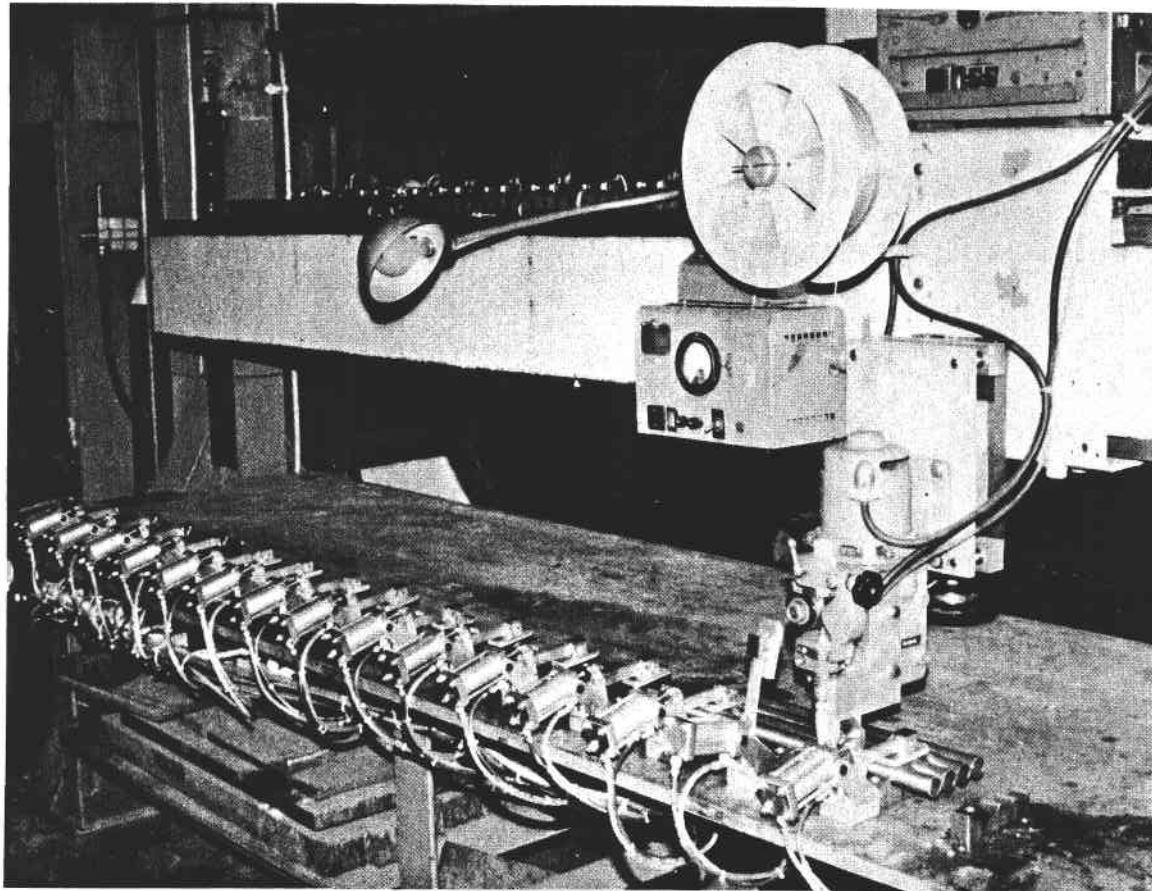


Figure 1.6 Overall View of Welding Set-Up Showing the Welding Head, Wire Reel, Controls, Cross-Beam Carriage, and Pneumatically Actuated Toggle Clamps

Several thicknesses of strip were considered and parametrically studied for thermal stresses. The results of the study indicated that a spacer strip 2.38 mm (3/32 in.) thick was best (Figure 1.7).

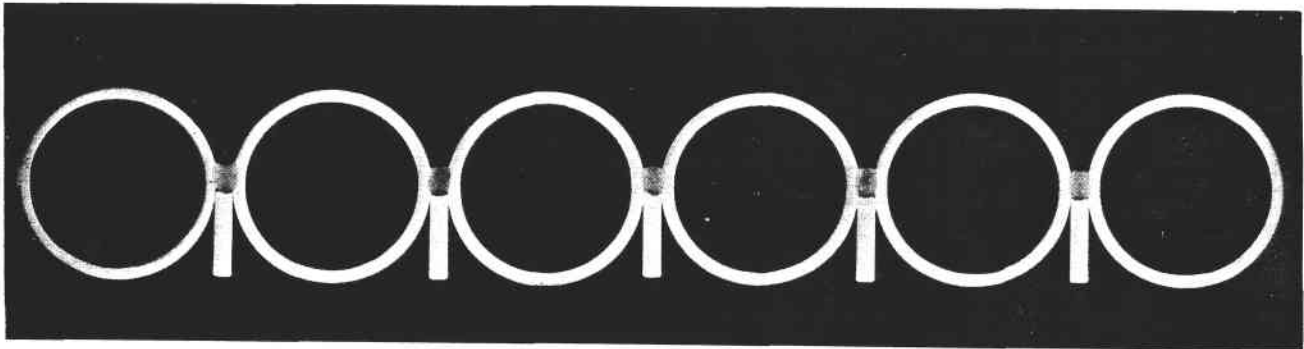


Figure 1.7 Cross Section of Welded Panel Tubes

Three 2.44-m (8-ft)-long development panels, 28 to 31 tubes wide, were fabricated using prototypical tubes. The first panel was fabricated from 25.4-mm (1-in.)-dia x 1.65-mm (0.065-in.)-wall thickness, Incoloy 800 seamless tubing and a 2.36-mm (0.093-in.) wide x 3.18-mm (1/8-in.) deep, rectangular, Incoloy 800 spacer strip. The fixture for welding the tubes was essentially the same as that used for trial welding. Scalloped support blocks with rectangular grooves for the spacer strip were spaced 0.15 m (6 in.) apart. Pneumatic clamps and end clamps restrained the tubes. Weights and 'C' clamps kept the in-process panel flat. Using welding parameters developed from trial welds, two-tube subassemblies were fabricated; these subassemblies were then joined to form a panel 30 tubes wide. A 31st tube was added separately.

Two major problems were encountered during this panel fabrication. First, the spacer strip often bowed in the vertical plane during welding, causing erratic welding behavior and also contributing to panel distortion. The second problem was differential expansion of adjacent tubes during welding, which contributed significantly to in-plane distortion in the form of "hour-glassing" (i.e., the panel was narrower at the midpoint than at the ends).

Aside from several fabrication changes, the second development panel was fabricated of the same materials and in the same manner as the first panel. The changes were intended to eliminate spacer strip bowing and to eliminate, or at least significantly reduce, the differential expansion of adjacent tubes. These fabrication modifications were partially successful; spacer strip bowing still occurred occasionally; panel distortion was decreased, but was still considered too great.

The third and last development panel was 28 tubes wide and was constructed of Type 304SS welded tubing of prototypical size and wall thickness and an 11.11-mm (7/16-in.)-deep x 2.34-mm (0.092-in.)-wide, rectangular, spacer strip, Type 304SS. We had to use Type 304SS in lieu of Incoloy 800 because of an unacceptable procurement delay for Incoloy 800 tubes and strip. Spacer strip depth was increased to retard bowing; the added mass reduced the differential expansion between the tube and the spacer strip and the added depth stiffened the strip in the vertical plane.

Distortion was eliminated by welding two-tube subassemblies, welding these into four-tube subassemblies, and then welding the four-tube subassemblies to

make up the 28-tube panel, thus maintaining symmetry in the process. In addition, the fixture for the third panel was modified and made more rigid to reduce panel distortion. No serious problems were experienced during the fabrication of the third panel (Figure 1.8). The strip bowing problem previously encountered was completely eliminated. Out-of-plane distortion was reduced considerably, and no measurable in-plane distortion was present.

We evaluated three methods for attaching support lugs to the panel (Figure 1.9). The first utilized integral welding of the lug and tubes--the lug legs replaced a section of the spacer strip. In the second, lug legs were butt-welded to the top of the spacer strips. In the third, the lug legs were placed inside and in contact with two adjacent spacer strips and were fillet welded to them. The third method was selected because it is easier to position and to weld.

Weld quality, tubewall penetration, and overall weld geometry were continuously monitored during trial welding and development panel fabrication by both destructive and nondestructive tests and examinations.

Strength tests were conducted at ambient temperature on specimens removed from the first development panel. The tests were designed to subject the specimens to loading and bending conditions exceeding those anticipated during normal panel operation. No cracks occurred in the welds or tubes. These tests showed that the tube-to-tube longitudinal welds were at least as strong as the tubes themselves.

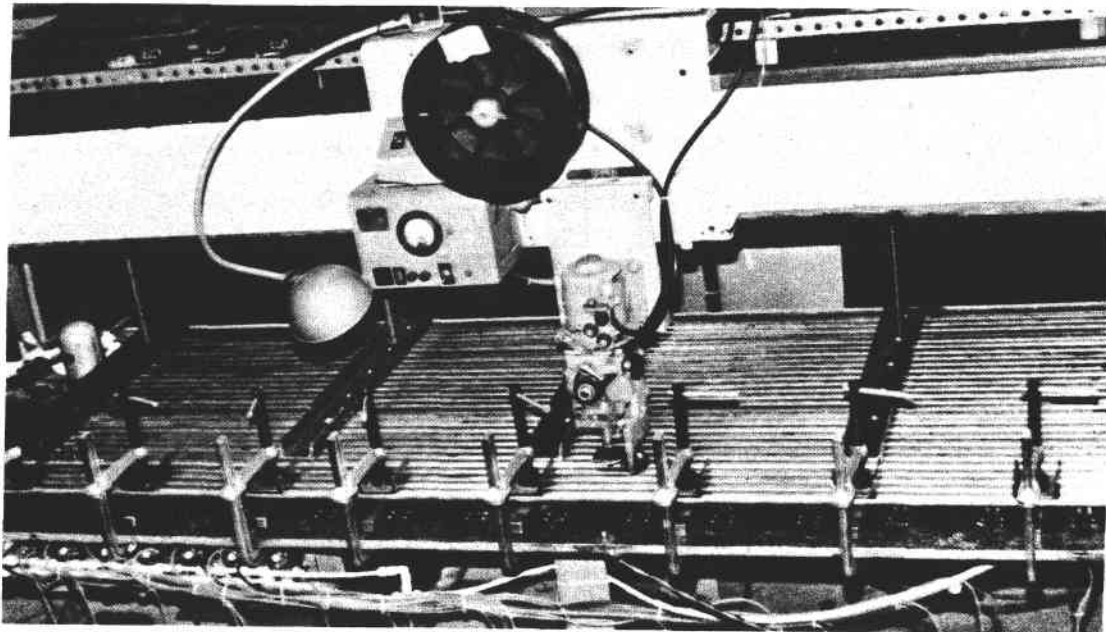


Figure 1.8 Welding of Third Development Panel

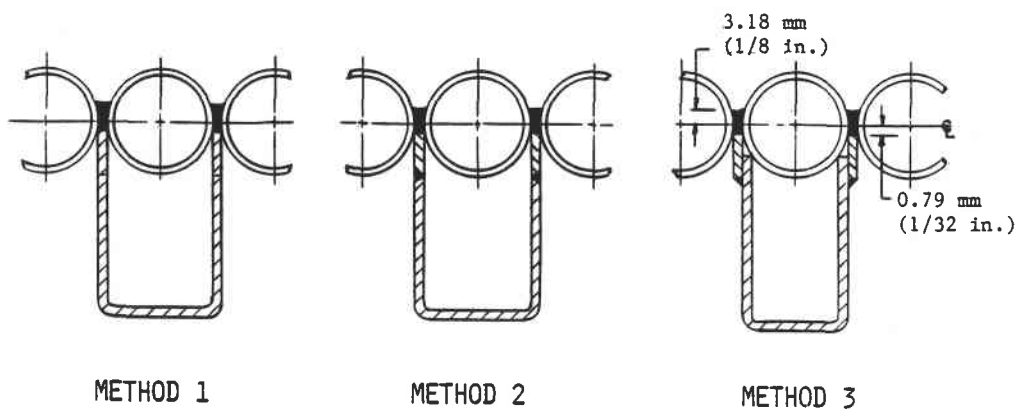


Figure 1.9 Support Lug Attachment Methods

Two prototypical panel lugs were subjected to a tensile strength test to show that the lug design would prevent tube distortion under maximum design load conditions and to determine the maximum load-carrying capacity of lugs and attachment welds. They successfully withstood loading to ≈ 32 times their design load.

Weld repairs were performed on 30.5-mm (1-ft)-long two-tube welded specimens prepared from Type 304SS tubes and spacer strip and Inconel 82 electrode. Repair welds were made using the same cross-sectional geometry, parameters, and fixtures employed to fabricate Panel 3, except that the original roller guide was replaced with a roller guide without a protruding lip. However, rewelding at these settings tended to distort the tubewalls, causing them to bow inward. Repair welds were made with a slightly colder setting (lower voltage) than used originally to minimize distortion.

Weld repairs should not be difficult provided the cavity created when the weld is removed is fairly precise dimensionally and the cavity is thoroughly cleaned. Weld repairs should be performed while the in-process panel is still in the welding fixture. A milling machine could be adapted to ride on the same cross-beam carriage as the welding head. The welding head used to make the original weld could also be used to make the repair weld with minimum modification.

Figure 1.10 shows the finished third development panel.

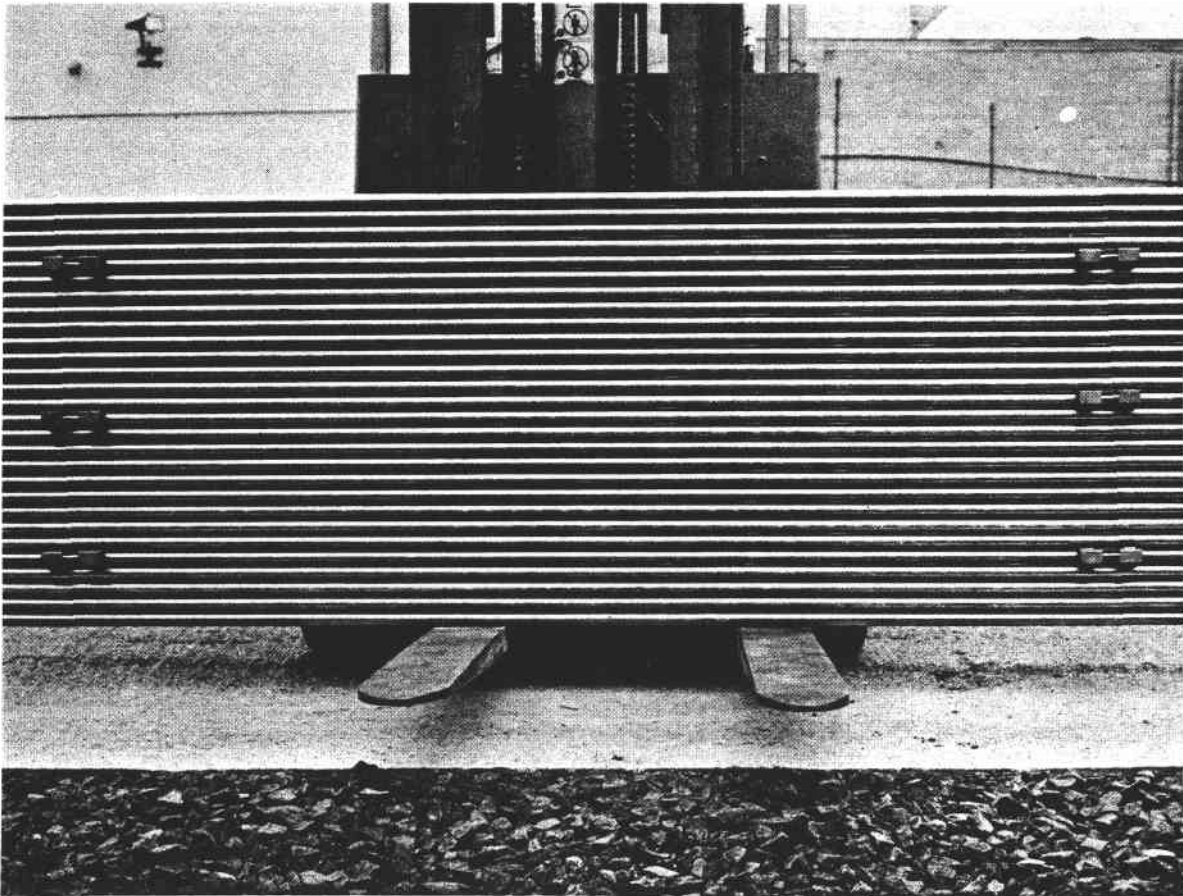


Figure 1.10 Third Development Panel Showing Support Lugs at Each End

1.6 WEIGHT AND COST ESTIMATES

The receiver weight breakdown--including salt and all components located above the tower--is shown in Table 1.6. Table 1.7 gives construction cost estimate in 1982 dollars for the complete RS including the receiver, concrete tower, riser and downcomer piping, feed pumps, and ancillary equipment.

Table 1.6 Receiver Weight

| | Weight | |
|---------------------------------------|--------------------|----------------------|
| | 10 ³ kg | (10 ³ lb) |
| Absorber panel modules | 109 | 240 |
| Roof and floor | 65 | 144 |
| Casing and insulation | 93 | 204 |
| Aperture door | 109 | 240 |
| Piping | 50 | 110 |
| Salt and air storage tanks | 57 | 126 |
| Controls and miscellaneous equipment | 25 | 56 |
| Platforms and ladders | 173 | 380 |
| Structural steel | 327 | 720 |
| Overhead crane | 50 | 110 |
| Normal charge of salt | <u>282</u> | <u>620</u> |
| Total estimated receiver weight (wet) | 1341 | 2950 |

Table 1.7 Construction Cost Estimate (\$ 1982)

| | |
|------------------------------|-------------------|
| Excavation and civil | 53,200 |
| Tower and foundation | 5,373,400 |
| Structural steel | 1,277,500 |
| Machinery and equipment | 10,743,700 |
| Piping and valves | 2,930,700 |
| Electrical | 308,100 |
| Instruments | 620,100 |
| Painting and insulation | 588,300 |
| Direct field costs | <u>21,895,000</u> |
| Indirect field costs | 437,700 |
| Total field costs | <u>22,332,700</u> |
| Total office costs | <u>2,283,000</u> |
| Total field and office costs | 24,615,700 |
| Contingency | 3,047,300 |
| Fee 8% | <u>2,213,000</u> |
| Total construction cost | 29,876,000 |

1.7 RECEIVER DEVELOPMENT

The major development issues for the molten salt receiver cover four broad areas:

- Design
- Performance
- Operation
- Molten salt and receiver technology

A considerable amount of development activity has been devoted to these issues and, based on these activities, a molten salt receiver can be designed, constructed, and operated. However, residual risks remain relating to absorber panel design, fabrication, and lifetime; receiver operation, availability, and maintenance; receiver performance and auxiliary power use; molten salt stability and corrosion; and creep-fatigue design requirements.

During Task 7 the verification status was reviewed, and verification options identified and correlated with the verification issues. Based on these reviews and a review of test capabilities and requirements, test programs for each of the major verification options and the risk reductions resulting from these programs were identified. Finally, a baseline test program with several options was proposed.

Candidate test program options include the following tests at Central Receiver Test Facility (CRTF) using the basic salt loop elements (with appropriate modifications) of the Molten Salt Electric Experiment (MSEE):

- Absorber Panel Test--of relatively short duration to verify the panel structural design and support system under realistic flux/temperature conditions.

- Cavity Test--would follow the panel test and be longer. It would investigate RS operability and utilization of available sunshine, overnight conditioning and door operation, outlet temperature control, receiver auxiliary power use, performance, and availability. Figure 1.11 gives the proposed SRE cavity configuration.
- Salt Loop Irradiated Panel Test--would be a small sub-loop of the MSEE and would have the capability for radiant heating of small test panel sections to investigate high bulk temperature/flux level phenomena in a tightly controlled environment.

In addition to these CRTF tests, a scale model section of the aperture door should be constructed and tested in an appropriate test facility. This test should include extensive thermal cycling of the door, seals, and trolley mechanism.

The cavity test was given first priority because it is the most comprehensive of the tests and it offers important information relating to operability and usability of insolation and receiver salt control experience--especially verification of physical modeling of salt flows. Additional data relating to aperture door and overnight conditioning, performance, and auxiliary power use will also be obtained; however, because of the limitations of instrumentation and scale, these data will provide verification of analysis methods more than verification of design.

The absorber panel test is second in priority because it will provide a meaningful scale test of the panel and its support structure and, by preheating the inlet salt, it is possible to operate the panel over the entire panel operating envelope. While past panel tests have provided only limited thermal/structural data because of limited test time and competing test objectives (e.g., control), this panel would be operated purely to simulate realistic

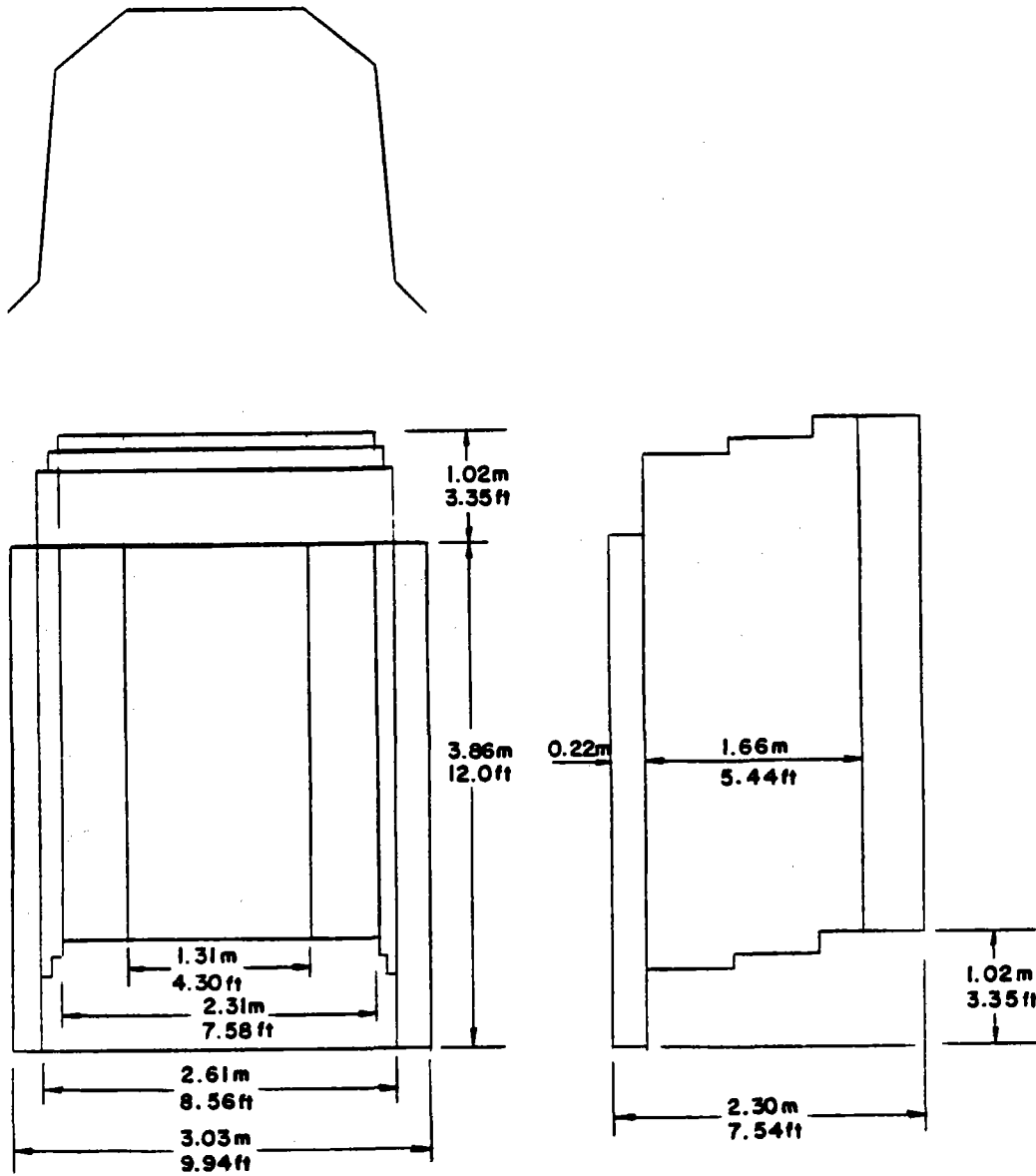


Figure 1.11 Schematic of the SRE Test Cavity

flux/temperature environments and cycles, which should maximize the useful thermal/structural design data obtained.

Supplementing the panel test is the salt loop panel section irradiation test. This test would use the mixed hot/cold tank salts bleed flows in panel test sections with radiant heaters. Both salt decomposition and panel corrosion would be monitored to provide better design criteria for receiver outlet pass flux limits.

Finally, included as an option is a subscale aperture door test. This test, which has not yet been designed, would supplement the cavity configuration door test in the same way that the panel test supplements the small-scale cavity panels. By combining the cavity test at small scale with the larger scale component tests (i.e., panel and door), both the overall integration and individual component problems can be investigated and corrected.

While these tests all offer useful information, detailed cost analyses of each are beyond the scope of this study. Of the tests considered, the most general and the one that will provide the best overall data is the cavity configuration test. The other tests, which are optional, can only be evaluated after better cost estimates are available.

UNLIMITED RELEASE
INITIAL DISTRIBUTION

U.S. Department of Energy (4)
Forrestal Building, Room 5H021
Code CE-314
1000 Independence Avenue, S.W.
Washington, D.C. 20585
Attn: C. Carwile
 H. Coleman
 F. Morse
 M. Scheve

U. S. Department of Energy (2)
P.O. Box 5400
Albuquerque, NM 87115
Attn: D. Graves
 J. Weisiger

U.S. Department of Energy
Solar One Field Office
P.O. Box 366
Daggett, CA 92327

U.S. Department of Energy (4)
1333 Broadway
Oakland, CA 94612
Attn: T. Heenan
 R. Hughey
 G. Katz
 W. Lambert

University of California
Environmental Science and Engineering
Los Angeles, CA 90024
Attn: R. G. Lindberg

University of Houston
Solar Energy Laboratory
4800 Calhoun
Houston, TX 77704
Attn: A. F. Hildebrandt

AMFAC
P.O. Box 3230
Honolulu, HI 96801
Attn: G. E. St. John

ARCO Power Systems
7061 S. University, Suite 300
Littleton, CO 80122
Attn: F. A. Blake

ARCO Power Systems
302 Nichols Drive
Hutchins, TX 75141
Attn: R. L. Henry

Arizona Public Service Company
P.O. Box 21666
Phoenix, AZ 85036
Attn: E. Weber

Babcock and Wilcox (3)
91 Stirling Avenue
Barberton, OH 44203
Attn: G. Grant
M. Seale
D. C. Smith

Badger Energy, Inc.
One Broadway
Cambridge, MA 02142
Attn: C. A. Bolthrunis

Bechtel Group, Inc.
P.O. Box 3965
San Francisco, CA 94119
Attn: G. W. Braun

Black & Veatch Consulting Engineers (3)
P.O. Box 8405
Kansas City, MO 64114
Attn: J. C. Grosskreutz
J. E. Harder
S. L. Levy

Boeing Engineering and Construction Company
P.O. Box 3707
Seattle, WA 98124
Attn: R. L. Campbell

California Energy Commission
1516 Ninth St., M/S 40
Sacramento, CA 95814
Attn: A. Jenkins

Combustion Engineering, Inc.
1000 Prospect Hill Road
Winsor, CT 06095
Attn: C. R. Buzzuto

El Paso Electric Company
P.O. Box 982
El Paso, TX 79946
Attn: J. E. Brown

Electric Power Research Institute (2)
P.O. Box 10412
Palo Alto, CA 94303
Attn: J. Bigger
E. DeMeo

Exxon Enterprises, Inc.
P.O. Box 592
Florham Park, NJ 07932
Attn: T. L. Guckes

Foster Wheeler Development Co. (2)
12 Peach Tree Hill Road
Livingston, NJ 07039
Attn: S. F. Wu
R. J. Zoschak

Georgia Institute of Technology
Atlanta, GA 30332
Attn: C. T. Brown

Gibbs and Hill, Inc.
393 Seventh Avenue
New York, NY 10001
Attn: J. J. Jimenez

Institute of Gas Technology
Suite 218
1825 K. Street, N. W.
Washington, D. C. 20036
Attn: D. Glenn

Jet Propulsion Laboratory
4800 Oak Grove Drive
Pasadena, CA 91103
Attn: M. Alpert

Los Angeles Department of Water and Power
Alternate Energy Systems
P.O. Box 111
111 North Hope St.
Los Angeles, CA 90051
Attn: D. Chu

Martin Marietta Aerospace
P.O. Box 179, MS L0450
Denver, CO 80201
Attn: H. Wroton

McDonnell Douglas Astronautics Company (3)
5301 Bolsa Avenue
Huntington Beach, CA 92647
Attn: R. L. Gervais
H. H. Dixon
C. M. Finch

Meridian Corporation
5113 Leesburg Pike
Falls Church, VA 22041
Attn: R. King

Olin Chemicals Group
120 Long Ridge Road
Stamford, CT 06904
Attn: F. N. Christopher
L. C. Fiorucci

Pacific Gas and Electric Company
77 Beale Street
San Francisco, CA 94105
Attn: R. Molano
R. E. Price

Pacific Gas and Electric Company
3400 Crow Canyon Road
San Ramon, CA 94526
Attn: C. Weinberg

Pioneer Mill Company (AMFAC)
P.O. Box 727
Lahaina, HI 96761
Attn: R. K. MacMillan

Rockwell International
Energy Systems Group
8900 De Soto Avenue
Canoga Park, CA 91304
Attn: T. Springer

Rockwell International
Rocketdyne Division
6633 Canoga Avenue
Canoga Park, CA 91304
Attn: J. M. Friefeld

Solar Energy Industries Association
1140 19th St. N.W.
Suite 600
Washington, D.C. 20036
Attn: C. LaPorta

Solar Energy Research Institute (2)
1617 Cole Boulevard
Golden, CO 80401
Attn: B. Gupta
R. Hulstram

Southern California Edison
P.O. Box 325
Daggett, CA 92327
Attn: C. Lopez

Southern California Edison
P.O. Box 800
Rosemead, CA 92807
Attn: J. N. Reeves
P. Skvarna

Stearns-Roger
P.O. Box 5888
Denver, CO 80217
Attn: W. R. Lang

Stone and Webster Engineering Corporation
P.O. Box 1214
Boston, MA 02107
Attn: R. W. Kuhr

Westinghouse Electric Corporation
Advanced Energy Systems Division
P.O. Box 10864
Pittsburgh, PA 15236
Attn: J. R. Maxwell

E. H. Beckner, 6000; Attn: V. Dugan, 6200
D. G. Schueler, 6220
J. V. Otts, 6222
R. S. Claassen, 8000; Attn: D. M. Olson, 8100
A. N. Blackwell, 8200
D. L. Hartley, 8300

C. S. Selvage, 8000A
C. Hartwig, 8244
M. E. John, 8245
R. C. Wayne, 8400; Attn: L. D. Bertholf, 8430
H. Hanser, 8440
R. L. Rinne, 8470

J. B. Wright, 8450
A. C. Skinrod, 8452
J. C. Swearngen, 8453
J. B. Wright, 8454 (Actg.)

Publications Division 8265, for TIC (27)
Publications Division 8265/Technical Library Processes Division, 3141
Technical Library Processes Division, 3141 (3)
M. A. Pound, 8024, for Central Technical Files (3)